Transient response mitigation using type-2 fuzzy controller optimized by grey wolf optimizer in converter high voltage direct current

I Made Ginarsa[1], I Made Ari Nrartha[1], Agung Budi Muljono[1], Osea Zebua[2]
[1]Department of Electrical Engineering, Faculty of Engineering, University of Mataram, Mataram, Indonesia
[2]Department of Electrical Engineering, Faculty of Engineering, Lampung University, Metro Lampung, Indonesia

Article Info

ABSTRACT

Long high voltage direct current (HVDC) transmission link is commonly used to transmit electrical energy via land or under-sea cable. The long HVDC avoids reactive power losses (RPL) and power stability problems (PSP). On the contrary, the RPL and PSP phenomena occur in long high voltage alternative current-link (HVAC) caused by the high reactive component in the HVAC-link. However, the HVDC produces a high and slow transient current response (TCR) on the high value of the up-ramp rate. Interval type-2 fuzzy (IT2F) control on converter-side HVDC is proposed to mitigate this TCR problem. The IT2F is optimized by grey wolf optimizer (GWO) to adjust input-output IT2F parameters optimally. The performance of IT2F-GWO is assessed by the minimum value of integral time squared error (ITSE), peak overshoot, and settling time of the TCR. The IT2FC-GWO performance is validated by the performance of IT2F control that is optimized by genetic algorithm (IT2F-GA) and proportional integral (PI) controller. Simulation results show that the IT2F-GWO performs better with small ITSE, low peak overshoot, and shorter settling times than competing controllers.

Corresponding Author:

I Made Ginarsa
Department of Electrical Engineering, Faculty of Engineering, University of Mataram
Majapahit Street, No. 62, Mataram 83125, Nusa Tenggara Barat, Indonesia
Email: kadekgin@unram.ac.id

1. INTRODUCTION

Transmission system is vital in a power system industry to deliver the electrical power/energy from power plants to consumers through distribution systems. Transmission systems categorized into alternating current (AC) and direct current (DC) types, according to the international electrical commission (IEC) standard regulation. Electrical energy delivered via high voltage direct current (HVDC) technology in modern transmission systems. This HVDC technology has intrinsic advantages such as being more favorable to install on very long distances for overhead or/and submersible transmissions, do not have reactive power losses, being feasible to connect for difference frequency systems (50/60 Hz), and having no stability issues appear in very long-distance transmission application. These advantages make the HVDC more convenient to implement than its competing (high voltage alternating current (HVAC)) technology. By using the newest power semiconductor technology, the AC/DC/AC converter process is more effective, efficient, and affordable in cost to be implemented. Moreover, ultra HVDC (UHVDC) transmission is a new technology that increases power capacity delivery, decreases electrical energy losses, and reduces of circuit-lines [1]. Some control and protection schemes for fault types in HVDC are provided in [2], [3]. A control scheme

regulating both the rectifier's voltage and current is designed to reduce transient response and increase the short-term transfer of electrical power capacity from the rectifier to the inverter in line commutated converter (LCC)-HVDC [4]. Super-conductor-damper device is applied in HVDC to minimize current and voltage oscillations effectively [5], and frequency limit control based on a modified frequency system is used to improve the stability of the sending side and avoid significant frequency-deviation [6]. A new small signal model (SSM) is designed by grounding impedance and proper control to damp the asymmetric direct-current mode in HVDC system [7], the SSM based on transfer function matrix mode is proposed to enhance stability of multiterminal HVDC [8], and the accurate SSM is used to reduce model complexity [9]. Cascading of AC-lines-outage is avoided by modulating close-loop control DC power in HVDC-line during the emergency period the HVAC line [10]. Fast-fault detection is applied, include on pole-and-line for both the single and double lines HVDC protection [11], and a commutation failure prevention model is designed by optimizing the value of resistance to minimize extinction angle in HVDC [12], a transient current is suppressed by supplementary control (SC) in rectifier HVDC [13], active disturbance rejection the SC is used to dampen oscillation in HVDC-line [14], and a novel SC is also applied to damp oscillation on maximum available power of extreme-weak AC-system [15].

Artificial intelligent (AI) applications in electrical and energy systems are introduced as follows: Machine learning is used to protect fault detection and classification scheme [16], and to search the fault location in HVDC systems [17]. Moreover, an artificial neural network (ANN) is used for fault detection and classification of the LCC-HVDC [18], to minimize transient stability for variation operating point [19], robust stability power on transmission [20] and direct current microgrid of shipyard system [21]. The other AI type that grows rapidly in electrical engineering application is fuzzy type-1 (including adaptive neuro-fuzzy inference system (ANFIS)) and interval type-2 fuzzy (IT2F) controls. The ANFIS controller is to maintain wind plant performance [22], enhance the dynamic performance of the 3-phase asynchronous motor [23], to faster the tracking speed and reduce static error at maximum [24]. The ANFIS scheme is built to regulate an inverter of HVDC [25], to stabilize a 3-bus power system (PS) [26], with the help of an IT2F-based power system stabilizer used to stabilize large scale PS [27]. The fuzzy and fuzzy-based direct torque control is implemented to maintain the dynamic performance of solar panels on the variation of radiation and temperature [24], and to reduce ripple induction motor [28], respectively. The IT2F based on a model reference controller and IT2F combined with digital signal processing are built to regulate a nonlinear system [29] and to improve the transient response of synchronous motor [30]. Some researchers have reported the advantages of HVDC system. However, the system is developed by power electronic devices and has some limitations. Therefore, high transient response and slow start-time are issues in the HVDC system. To overcome these problems, some methods are proposed to reduce transient responses, as follows: Feed-forward compensator on AC-to-DC converter in DC distribution system [31], the ANN embedded by machine learning on converter/inverter switching [32], triangular source signal on DC-to-DC buck converter [33], internal feed-forward [34] and [35] feed-forward compensators on DC-to-DC converter.

On the other hand, optimization method (OM) is developed into two classes: based on mathematical programming and metaheuristic algorithm [36]. The metaheuristic algorithms are generally divided into four categories according to their inspiration sources [37]: i) genetic evolution algorithms. Evolutionary mechanisms in biology inspired this algorithm, and these algorithms imitate genetic evolution properties in nature. Four mechanism stages occur in these processes such as: reproduction, mutation, recombination, and selection. These algorithms mimic tree competition to optimize sunlight directly and food in the forest. Tree growth algorithm (TGA) is developed in intensification and diversification phases. The best trees are developed by sunlight quality sufficiency, good chromosomes' gens with related to water and healthy food, which are determined in the intensification phase. Diversification phase is performed by removing the worst solution, instead of them by generating the solution randomly, and reproducing more seedlings; ii) swarm intelligence. These algorithms mimic the animal habit of food foraging or scheduling. Improved northern goshawk optimization is one of the animal behavior based algorithm and this algorithm is applied in [38], where an adaptive parameter is created using the levy flight concept. So, this mechanism guarantees a smooth transition from exploration to exploitation phases to maintain global optimization further. A giant trevally optimizer also uses the animal in search foraging potential. A dynamic TGA version is applied to manage cost and computational efficiencies for load scheduling on cloud computing [39]; iii) human activity algorithms. These algorithms are based on the human activities in teaching-learning between the teacher and students in class. This algorithm is used to decrease cost on solar cell power plant [40]. Also, queuing search algorithm is inspired by queuing behavior of some consumers to pay their shopping goods in a super market cashier [41]; and iv) algorithms that developed from other sources, such as scientific-based algorithm [42]. This optimization method is built based on a crystal structure algorithm that inspired from crystal formation based on addition of basis and lattice points. Moreover, this method has tested successfully using mathematical test standards and synchronous optimal pulse width modulation on n-level inverters (where, n=3−13) of medium voltage for electric drives. The OM is built using different model and applied in

electrical engineering, also growing rapidly, likes: two-stage economic dispatch operation using improved-chaotic brain-storm OM in integrated energy system [43], chaotic based on predator-prey brain-storm and enhanced teaching-learning based OMs are effectively to minimize real power losses in power systems [44], [45], and particle swarm optimization (PSO) is used for optimal location of solar and wind turbine on distribution system [46]. The PSO is applied to improve the stability of wind-farm HVDC system [47] on photovoltaic (PV) tracking [48], and PSO-gravitational search algorithm is implemented to optimize the protection relay of distributed generation [49]. Genetic algorithm OM based on sliding-mode scheme is used to enhance the dynamic stability of source voltage converter HVDC in considering wide range operating conditions [50]. Bacterial foraging OM is applied in capacitor-run motor [51], and grey wolf optimizer (GWO) is developed to estimate input-output parameters power plant [52] and to compute the optimal shape and size in design of 800 kV transformer of HVDC system [53].

The transient current response (TCR) problem has been paid more attention in HVDC [4], [31], [35], and their solutions using some methods are explained before. Nevertheless, IT2F optimized by GWO method has never been implemented to suppress the TCR problem. To bridge this scheme′s vacuum, we propose the IT2F control optimized by the GWO to mitigate the transient current on a start-up period in the converter of HVDC. This manuscript is organized as follows: HVDC and IT2F models are explained in section 2. Furthermore, section 3 explores the procedure to design and obtain GWO parameters. Next, results of proposed control are analyzed and discussed in section 4. Finally, a conclusion is provided in section 5.

2. HIGH VOLTAGE DIRECT CURRENT AND TYPE-2 FUZZY CONTROL

A HVDC transmission system is a popular method to transmit large of electric power to avoid more reactive power losses, especially on long-range transmission. The model is developed by: an ideal source, filter, and rectifier at sending end, a 300 km long-distance DC-line, inverter, filter, and an ideal source at receiving end. The HVDC system follows from [54]. In HVDC operation, the role of firing angle regulation of converter HVDC is very important to adjust the current (power) flowing from the sending to the receiving end. The HVDC transmission system and implementation of IT2F-GWO control on its converter are shown in Figure 1(a). The information process in IT2F is illustration in Figure 1(b). Figure 2(a) shows the Input 2 membership function (MF). The Gaussian MF with 3-upper (mf1U, mf2U, and mf3U for the upper MFs) and 3-lower (mf1L, mf2L and mf3U for the lower MF), respectively. Variables dEi and $\mu(dEi)$ are the derivative of fuzzy control′s current error signal (Input 2) and their degree of respective MFs. Figure 2(b) illustrates the optimization process of input-output parameters using the GWO technique. The Kin_1, Kin_2 and K_{out} are parameter Input 1, 2, and Output, respectively. The Ei, t and αSC are current error signal (Input 1), time multiplier, and supplementary control (Output) signal.
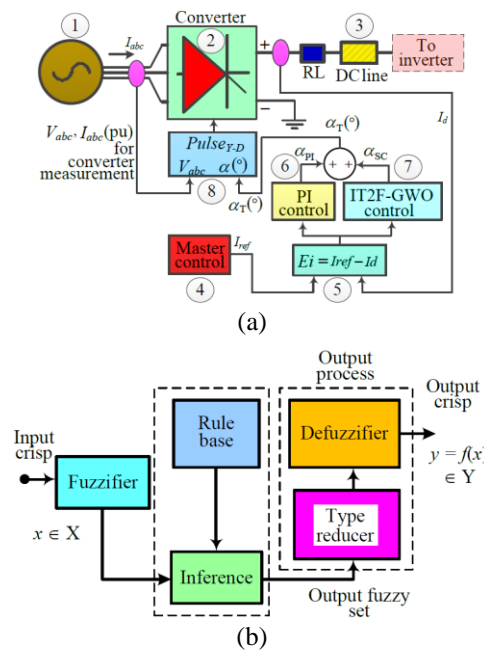

(a)

(b)

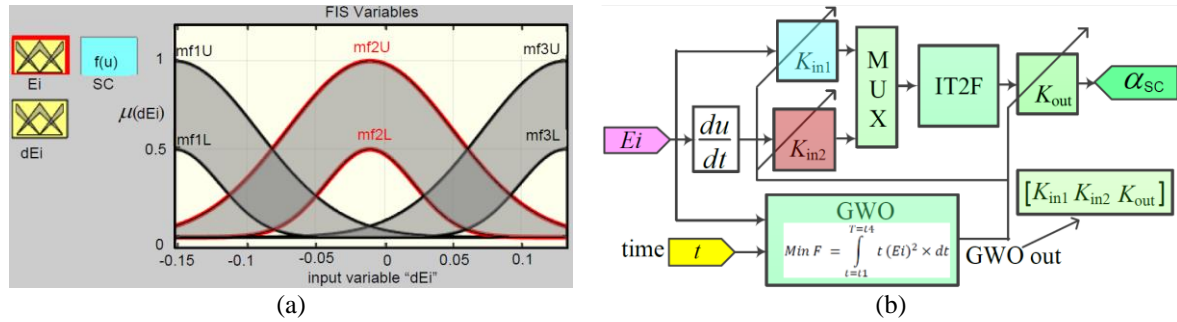Figure 1. Diagram block of (a) proposed control (IT2F-GWO), (b) interval type-2 fuzzy for converter HVDC

Figure 2. The IT2F-GWO model control, (a) three membership function type Gaussian for Input 2 (dEi) and (b) adjusting value of input-output parameters using GWO technique

3.   GREY WOLF OPTIMIZER

A new model optimization algorithm introduced in [55] is one of the common intuitive algorithm based on population. The model is to mimic the grey wolf's behavior in hunting their prey in the natural wild. The wolves generally have a social life with strongly rigid leadership and hierarchy. The leadership in the grey wolf group is categorized in four orders: α (alpha), β (beta), δ (delta), and ω (omega). This group will be built to explore and exploit search-hunting areas. The GWO has tuned parameter requirements such as population size, iteration, and optional control vector. The top hierarchy is *alpha* wolves, which govern the group's function, are responsible for decision-making, and manage the group on social life and hunting field. The second order is *beta* wolves that serve as the sub-ordinate and advisor for other wolf orders. Figure 3(a) shows the grey wolf social hierarchy in prey hunting. To describe the grey wolves while hunting prey, we explore this mechanism in four stages: Encircling, hunting, attacking, and search-for-prey.

3.1. Encircling-prey stage

When grey wolves find the potential prey to be hunted, they will encircle the prey immediately. In the encircling-prey stage, the mathematical model of the grey wolf behavior is illustrated by (1), (2).

$$\vec{D} = |\vec{C}.\vec{X}_{pr}(it) - \vec{X}_{gw}(it)| \tag{1}$$

$$\vec{X}_{gw}(it+1) = \vec{X}_{pr}(it) - \vec{A}.\vec{D} \tag{2}$$

where it, ($\vec{A}$ and $\vec{C}$), $\vec{X}_{pr}$ and $\vec{X}_{gw}$ are the current iteration, coefficient vectors, position vector of prey and position vector of the grey wolf, respectively. Furthermore, the vectors ($\vec{A}$ and $\vec{C}$) are computed using (3), (4):

$$\vec{A} = 2\vec{a}.\vec{r}_1 - \vec{a} \tag{3}$$

$$\vec{C} = 2.\vec{r}_2 \tag{4}$$

where vector component $\vec{a}$ is decreased linearly from 2 until 0 throughout iterations. The $r_1 and r_2$ are defined as random vectors in the range [0,1].

3.2. Hunting-prey

The *alpha* commonly leads and guides the other wolves in this hunting stage. Suppose the *alpha*, *beta*, and *delta* wolves know the potential target (prey) position better. Firstly simulation, the first three best solutions ($\vec{X}_{alpha}, \vec{X}_{beta},$ and $\vec{X}_{delta}$) are achieved, and these results are saved. Next step is to obligate the other agents including omegas, to update their position following to the position of the best search agents. These processes can be formulated as (5), (6), and (7).

$$\vec{D}_{alpha} = |\vec{C}_1.\vec{X}_{alpha} - \vec{X}_{gw}|; \vec{D}_{beta} = |\vec{C}_2.\vec{X}_{beta} - \vec{X}_{gw}|; \vec{D}_{delta} = |\vec{C}_1.\vec{X}_{delta} - \vec{X}_{gw}| \tag{5}$$

$$\vec{X}_1 = \vec{X}_{alpha} - \vec{A}_1.(\vec{D}_{alpha}); \vec{X}_2 = \vec{X}_{beta} - \vec{A}_2.(\vec{D}_{beta}); \vec{X}_3 = \vec{X}_{delta} - \vec{A}_3.(\vec{D}_{delta}) \tag{6}$$

$$\vec{X}_{gw}(it+1) = \frac{\vec{X}_1 + \vec{X}_2 + \vec{X}_3}{3} \tag{7}$$

The GWO allows its search agents to newer (update) their position based on the *alpha*, *beta*, and *delta*, further attacking the prey. The search agent updates its position according to *alpha*, *beta*, and *delta* in 2-dimension, as shown in Figure 3(b).

3.3. Attacking-prey

The attacking stage is done by a group hunting grey wolves when a target is stopped at a certain location. A mathematical variable $\vec{a}$ is used to approach the prey model, and the value of $\vec{a}$ decreases when the grey wolves toward approach the prey. The value of $\vec{a}$ is decreased from 2 to 0 during iteration processes. Where values of $\vec{A}$ are the random number in the range $[-2a, 2a]$, consequently, this condition decreases the fluctuation range of $\vec{A}$. For the values of $\vec{A}$ are in range $[-1, 1]$, the next position of a search agent is in any position between its current and the prey position. For wolf's positions in range $|A| < 1$, the wolves are ready and forced to attack the prey, as shown in Figure 3(c). We can call this situation "they convergent to attack the target (prey)".

3.4. Search-for-prey

Besides attacking mode, search-for-prey is an important step during the hunt process. Grey wolves search the prey according to the member (*alpha*, *beta*, and *delta*) positions participating in hunting the prey. The grey wolves spread out each other, and their positions will get far away. The divergence model of search-for-prey occurs when the value of $\vec{A}$ more than 1 or less than -1; ($|A| > 1$). This situation is named the search agent to diverge from the prey and is described in Figure 3(d). Furthermore, the GWO also uses vector $\vec{C}$ to provide random weights for the prey to emphasize ($C > 1$) or de-emphasize ($C < 1$) that is associated with the prey distanc, as defined in (4). GWO uses this mechanism to find more random behavior during optimization, favoring exploration and avoiding local minima.
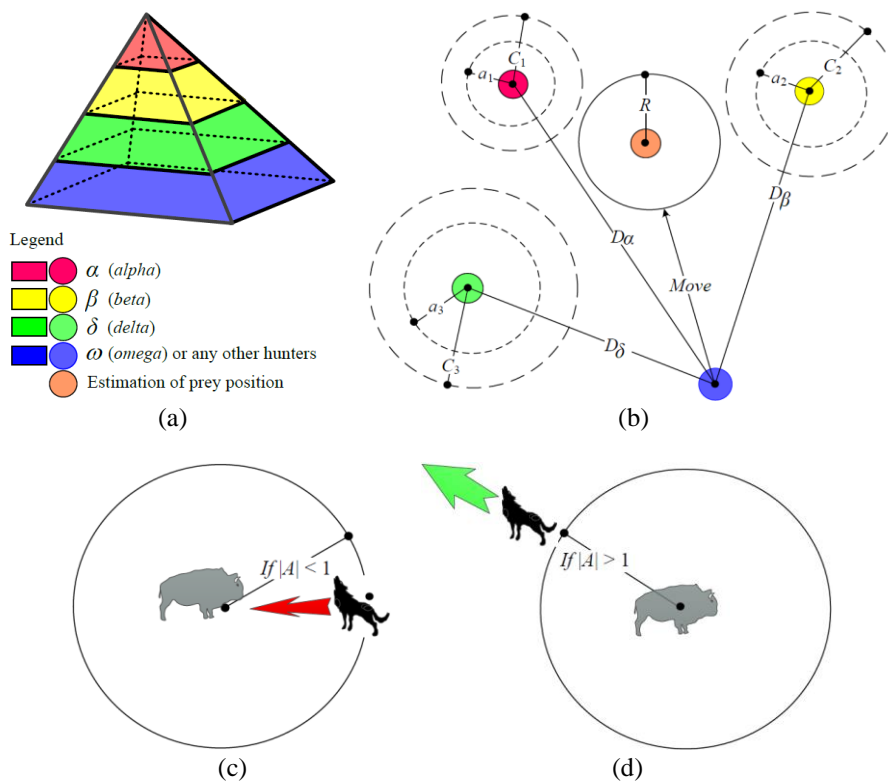

Figure 3. Grey wolf structure and member positions, (a) social hierarchy, (b) update position mechanism, (c) attacking the prey directly, and (d) searching for new prey

The procedure of governing the GWO algorithm is developed as follows: first time is to initialize the grey wolf population, parameters α, A, C, and maximum iteration (*it*). While the iteration (*it*) less than maximum iteration and the loop *i*: from 1 to the number of search agents, update the values of respective

search agents (X_{alpha}, X_{beta}, and X_{delta}). Call/run the HVDC system equipped by proposed controller in Simulink model. Calculate the fitness of each search agent and evaluate the fitness value of search agents. For the fitness of search agents is smaller than the specification fitness value, then update the *alpha*, *beta* and *delta* scores, or discard the result. Next, update the position of search agents including the *omega* and calculate the best *alpha* for score and position of current iteration. Finally, print the best *alpha* for score and position when the maximum iteration is achieved. The GWO pseudo code is described in Figure 4(a). Also, the GWO algorithm is illustrated in Figure 4(b).
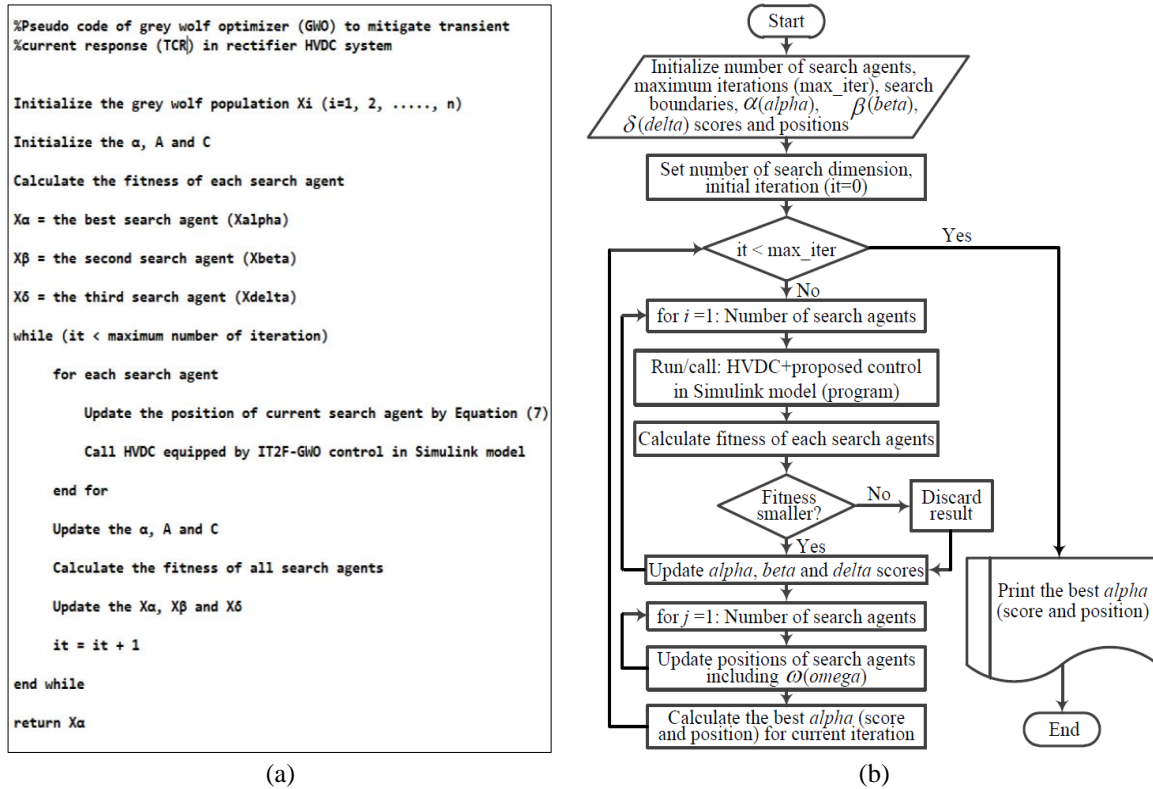

Figure 4. Proposed control procedure, (a) pseudo code and (b) flowchart

3.5. Fitness function building

In an optimization algorithm, it is very important to obtain the fitness (object) function of the system response. The input signal is the current reference ($Iref$) that this signal is used to trigger the thyristor gate in converter HVDC system. The HVDC's starting procedure and the current reference pattern in this research follow the pattern in [54]. The set point (desired response) is the current reference and response of the direct current (Id) the HVDC system at start-up time. The illustration of building the fitness function from the response is shown in Figure 5. Figure 5 and (8) show that the F_{fit} is the sum of F_1, F_2, and F_3. The performance of the controller is developed based on integral time squared error (ITSE) criteria of current reference and direct current response. The fitness function is built into formulating:

$$\text{Minimum } F_{fit} = F_1 + F_2 + F_3 = \sum_1^3 F_m \tag{8}$$

$$F_m = \int_{t_m}^{t_{m+1}} t \times (Ei)^2 dt = \int_{t_m}^{t_{m+1}} t \times (Iref - Id)^2 dt \tag{9}$$

The $Ei, Iref$ and Id are current error, current reference, and direct current signals, respectively. Integer number m is 1, 2, and 3. Suppose that for $m=1$, time periods are defined as follows: $t_m = t_1, t_{m+1} = t_2; m = 2, t_m = t_2, t_{m+1} = t_3; and \ m = 3, t_m = t_3, t_{m+1} = t_4$. The minimum value of F_{fit} is used to examine the control performance. The F_1, F_2 and F_3 are results of integral time and squared area between direct current and current reference at each time periodic, respectively.
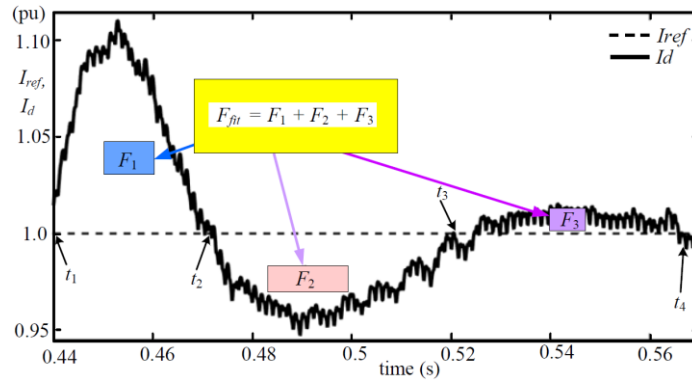
Figure 5. Fitness function for direct current response of converter HVDC system

4. SIMULATION RESULTS AND DISCUSSION

The IT2F-GWO controller performance is assessed by increasing the load from 0 to 10% loading on receiving-end transmission line (increasing up-ramp final-value, $Iref$ from 1.0 to 1.1 pu) in 11 scenarios. Every scenario (loading condition) is run in ten times for GWO and GA optimization. Up-ramp rate is taken on 25 pu/s. In this scenario, the master control parameters were set as follows: Up-ramp final-value ($Iref$), Up-ramp, and Up-ramp at 1 pu, 25 pu/s, and 4 s. Simulation is performed on server computer Xeon E5-2630, 8 Cores, 15 Mb Cache, and 16-thread hardware. Also, we use MATLAB/Simulink software [56]. The PI controller on default setting [54] is used to validate the proposed control results.

4.1. Simulation set-up of the GWO

The GWO parameters were adjusted to obtain the optimized control: Search agent, number of variables, the lower and upper bounds of variables, and maximum iteration. The search agent is given at the values of 10, 15, 20, 25, 30, 35, and 40. There are three kinds of variables (Kin_1, Kin_2 and K_{out}) with [10 10 1] and [0.01 0.01 0.01] chosen as the upper and lower bounds of variables, Maximum iteration is taken at 50 iterations. To validate the procedure and result of the GWO, the HVDC control was also optimized by genetic algorithm (GA). The GA method used in this research is 'optimtool' provided by [56]. The setting of GA parameter is as follows: Population type: double vector; population size was taken at 10, 15, 20, 25, 30, 35, and 40; creation function: uniform; initial range: [−10 10]; selection function: tournament. Furthermore, the iteration is taken at 50 generations. Comparison of convergence (ITSE) curves from the GA and GWO methods are given in Figure 6.
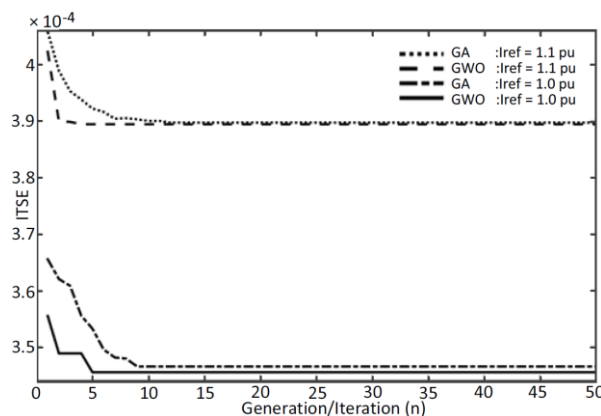

Figure 6. Convergence curve of GA and GWO for current reference at 1 and 1.1 pu run in 50 iterations

4.2. Performance of proposed control

The ITSE of respective transient current response (TCR) is used to assess controller's performance. The ITSE of controllers are compared and listed in Table 1. The ITSE for the PI, IT2F-GA, and IT2F-GWO

was obtained at (4.9256, 3.4649 and 3.4547)×10⁻⁴, respectively. The simulation result of the PI, IT2F-GA, and proposed controller (IT2F-GWO) for (current reference, $Iref$ =1 pu) is described in Figure 7(a). To distinguish the results of IT2F-GA and IFT2-GWO, the block ′abcd′ is mapped into block ′ABCD′ as shown in Figure 7(b). It is clear that in block ′ABCD′ of Figure 7(b), we see the direct current (Id) of the IT2F-GA and IT2F-GWO achieved peak value (M_{po}), which are labelled by M_{po-1} and M_{po-2}, respectively. Next, the current reference was increased to 1.01 pu, and the ITSE was monitored at (4.9794, 3.4981, and 3.4742)×10⁻⁴ for the PI, IT2F-GA, and IT2F-GWO controllers, respectively. The current reference was increased to 1.02, 1.03, until 1.1 pu. For the current reference at 1.1 pu, the ITSE performance is monitored at (5.3614, 3.8971 and 3.8819)×10⁻⁴ for the PI, IT2F-GA, and IT2F-GWO controllers. Moreover, the average value of the ITSE from this scenario was obtained at (5.1704, 3.6711 and 3.6528)×10⁻⁴ for the PI, IT2F-GA, and IT2F-GWO controllers.

Table 1. ITSE performance of the proposed control for 0-10% load increased and in 50 iterations

$Iref$	PI	IT2F-GA	IT2F-GWO				
(pu)	ITSE (×10⁻⁴)	ITSE (×10⁻⁴)	ITSE (×10⁻⁴)	Search agent	Kin_1	Kin_2	K_{out}
1	4.9256	3.4649	3.4547	15	0.5047	0.2260	0.9145
1.01	4.9794	3.4981	3.4742	25	0.9575	1.0644	0.6743
1.02	5.0433	3.5462	3.5195	30	1.1786	0.3862	0.6698
1.03	5.0686	3.5609	3.5485	35	1.1176	0.4921	0.6702
1.04	5.1447	3.6365	3.6027	15	0.5317	0.01	0.7911
1.05	5.2284	3.6629	3.6614	25	0.5991	0.01	0.7956
1.06	5.2326	3.7213	3.6984	35	0.5729	0.8790	0.8039
1.07	5.2509	3.7721	3.7326	25	0.01	1.4876	0.8097
1.08	5.3073	3.7932	3.7775	25	0.2587	0.5395	0.8347
1.09	5.3327	3.8289	3.8293	25	0.4958	0.1671	0.8561
1.1	5.3614	3.8971	3.8819	35	0.01	0.3400	0.7882
average	5.1704	3.6711	3.6528				
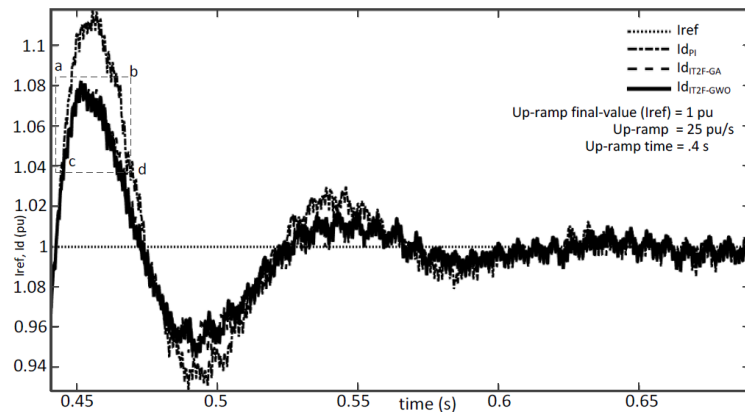
(a)
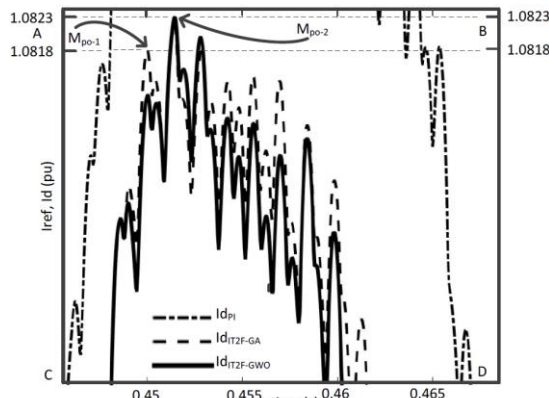
(b)

Figure 7. Simulation result by proposed control for final-value ($Iref$) at 1.0 pu, (a) response improvement of direct current and (b) magnification of the block ′abcd′ to the block ′ABCD′

Figure 8(a) illustrates the simulation result for the current reference at 1.1 pu. Illustration of the direct current (*Id*) result in block ′efgh′ is magnified to block ′EFGH′ to differentiate the direct current of IT2F-GA and IT2F-GWO is depicted in Figure 8(b). In the block ′EFGH′ of the Figure 8(b), the direct current of the IT2F-GA and IT2F-GWO achieved peak value (M_{po}). The peak values for the IT2F-GA and IT2F-GWO are marked by labels M_{po-3} and M_{po-4}, respectively. It is shown that the peak overshoot of the IT2F-GWO is lower than the IT2F-GA peak overshoot. From this scenario, the proposed control gives better result on mitigating the current response than other competing controllers.
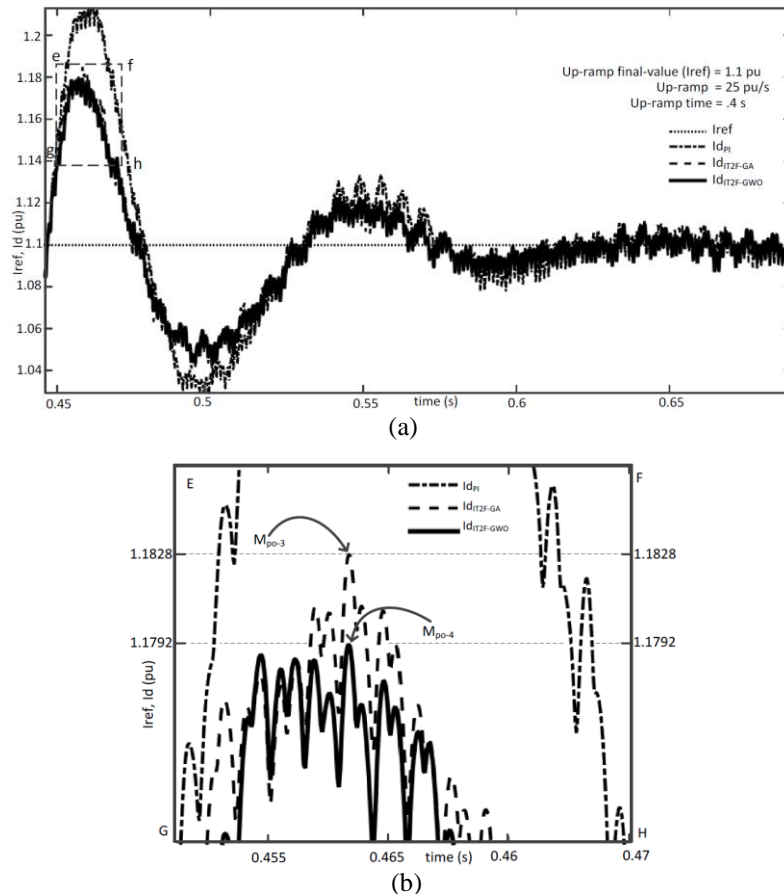

(a)

(b)

Figure 8. The IT2F-GWO controller response for 1.1 pu, (a) the IT2F-GWO response enhancement compared to other controllers and (b) to distinguish the peak overshoot of the IT2F-GA (M_{po-3}) and IT2F-GWO (M_{po-4}) controllers, so the block ′efgh′ is clarified to the block ′EFGH′

Simulation results of peak (maximum) overshoot (M_{po}) and settling time (t_s) for the current reference scenario are also monitored to assess the effectiveness of the proposed controller compared the others. For the current reference at 1 pu, the M_{po} was at 1.1182 (11.82), 1.0818 (8.18), and 1.0823 (8.23) pu (%) for the PI, IT2F-GA, and IT2F-GWO, respectively. The settling time was obtained at time of 0.605, 0.5679, and 0.5673 s for the PI, IT2F-GA, and IT2F-GWO controllers. Next, for the current reference was at 1.01 pu, the peak overshoot was achieved at 1.1271 (11.59), 1.0919 (8.11), and 1.0889 (7.81) pu (%) for the PI, IT2F-GA, and IT2F-GWO. The settling time was at time 0.6074, 0.5703, and 0.5691 s for the PI, IT2F-GA, and IT2F-GWO. The simulation was also done for the current reference at 1.02, 1.03 pu, etcetera; the complete results of this scenario are listed in Table 2. Finally, for the *Iref* at 1.1 pu, the peak overshoot was at 1,214 (10.36), 1.1828 (7.53), and 1.1792 (7.2) pu (%) for the PI, IT2F-GA, and IT2F-GWO, respectively. The settling time (t_s) was settled at time 0.6219, 0.6103, and 0.6075 s for the PI, IT2F-GA, and IT2F-GWO controllers. Based on the results in this scenario, we show the proposed controller gives a smaller the integral time squared error (ITSE) for current reference and direct current compared to the other controllers. The peak overshoots and settling times of the proposed control are smaller and shorter than the others. It is shown that the proposed gives better result than the others for the increasing of current reference scenario.

Table 2. Peak overshoot and settling time performances of the proposed control

Iref (pu)	PI		IT2F-GA		IT2F-GWO	
	M_{po} [pu (%)]	t_s (s)	M_{po} [pu (%)]	t_s (s)	M_{po} [pu (%)]	t_s (s)
1	1.1182 (11.82)	0.605	1.0818 (8.18)	0.5679	1.0823 (8.23)	0.5673
1.01	1.1271 (11.59)	0.6074	1.0919 (8.11)	0.5703	1.0889 (7.81)	0.5691
1.02	1.1431 (12.07)	0.6081	1.0996 (7.8)	0.5761	1.099 (7.75)	0.5738
1.03	1.154 (12.04)	0.6109	1.1164 (8.39)	0.5794	1.1092 (7.69)	0.5762
1.04	1.1662 (12.13)	0.6113	1.1255 (8.22)	0.5819	1.1214 (7.83)	0.5793
1.05	1.1735 (11.76)	0.6135	1.1362 (8.21)	0.5872	1.1357 (8.16)	0.5846
1.06	1.1816 (11.47)	0.6148	1.1473 (8.24)	0.5939	1.1442 (7.94)	0.5874
1.07	1.1899 (11.21)	0.6156	1.1586 (8.28)	0.5948	1.1524 (7.7)	0.5913
1.08	1.1966 (10.8)	0.6173	1.165 (7.97)	0.5985	1.1623 (7.62)	0.5937
1.09	1.2074 (10.77)	0.6207	1.171 (7.43)	0.6046	1.1705 (7.39)	0.5982
1.1	1.214 (10.36)	0.6219	1.1828 (7.53)	0.6103	1.1792 (7.2)	0.6075

5. CONCLUSION

Interval type-2 fuzzy-grey wolf optimizer (IT2F-GWO) is proposed on converter side to mitigate the HVDC-link system′s TCR at start time. The IT2F is developed by knowledge-based of the designer with Gaussian MF on two inputs and linear MF one output at first time. Next, three input-output parameters of the IT2F are adjusted by the GWO to determine the optimal value by assigning the TCR′s ITSE. To obtain the optimal IT2F parameters, GWO is run on 50 iterations with search agents increased from 10-40 search agents. Simulation result show that the ITSE of the proposed control is achieved at 3.4547×10^{-4} for up-ramp final-value (*Iref*=1 pu; *Up-ramp rate*=25 pu/s). The simulation result of the proposed control is also compared to IT2F optimized by genetic algorithm (IT2F-GA) and PI control to validate its result. So, the IT2F-GA and PI give the ITSE at $(3.4649$ and $4.9256) \times 10^{-4}$, respectively. The maximum peak overshoot (M_{po}) of direct current is obtained at the values of 1.1182 (11.82%), 1.0818 (8.182%), and 1.0823 (8.23%) for the PI control, IT2F-GA, and IT2F-GWO. The settling time is achieved at 0.605, 0.5679 and 0.5673 s for the PI control, IT2F-GA, and IT2F-GWO. When the *Iref* increased toward 1.1 pu, the respective controllers give the ITSE at $(5.3614, 3.8971,$ and $3.8819) \times 10^{-4}$ for the PI, IT2F-GA, and IT2F-GWO controllers. Simulation results in all scenarios give the average value of ITSE at $(5.1704, 3.6711,$ and $3.6528) \times 10^{-4}$ for the PI, IT2F-GA, and IT2F-GWO. The maximum peak overshoot is obtained at 1,214 (10.36%), 1.1828 (7.53%), and 1.1792 (7.2%) for the PI, IT2F-GA, and IT2F-GWO. The settling time is at a time of 0.6219, 0.6103 and 0.6075 s for the PI, IT2F-GA, and IT2F-GWO, respectively. The proposed controller can mitigate the TCR of converter HVDC transmission with better performance than the other controllers.

REFERENCES

[1] D. Huang, Y. Shuu, J. Ruan, and Y. Hu, "Ultra high voltage transmission in China: Developments, current status and future prospects," *Proceedings of the IEEE*, vol. 97, no. 3, pp. 555–583, 2009, doi: 10.1109/JPROC.2009.2013613.

[2] Y. Zhang, Y. Li, J. Song, X. Chen, Y. Lu, and W. Wang, "Pearson correlation coefficient of current derivatives based pilot protection scheme for long-distance LCC-HVDC transmission lines," *International Journal of Electrical Power and Energy Systems*, vol. 116, no. May 2019, 2020, doi: 10.1016/j.ijepes.2019.105526.

[3] M. Muniappan, "A comprehensive review of DC fault protection methods in HVDC transmission systems," *Protection and Control of Modern Power Systems*, vol. 6, no. 1, pp. 1–20, 2021, doi: 10.1186/s41601-020-00173-9.

[4] D. H. Kwon, Y. J. Kim, and S. I. Moon, "Modeling and analysis of an LCC HVDC system using DC voltage control to improve transient response and short-term power transfer capability," *IEEE Transactions on Power Delivery*, vol. 33, no. 4, pp. 1922–1933, 2018, doi: 10.1109/TPWRD.2018.2805905.

[5] N. Kimura, T. Funaki, and K. Matsu-Ura, "Damping of current oscillation in superconductive line applied for high voltage direct current transmission system," *IEEE Transactions on Applied Superconductivity*, vol. 3, no. 1, pp. 223–225, 1993, doi: 10.1109/77.233711.

[6] H. Zhang, K. Wei, Y. Wei, and H. Zhu, "Emergency power control strategy of HVDC FLC based on modified SFR model in islanded HVDC sending system," *International Journal of Electrical Power and Energy Systems*, vol. 142, no. PA, Art. no. 108314, 2022, doi: 10.1016/j.ijepes.2022.108314.

[7] J. Serrano-sillero and M. Angeles, "Small-signal stability analysis of the asymmetrical DC operation in HVDC networks," *Electric Power Systems Research*, vol. 214, no. July 2022, 2023, doi: 10.1016/j.epsr.2022.108942.

[8] X. Chen, Y. Liang, G. Wang, H. Li, B. Li, and Z. Guo, "A control parameter analysis method based on a transfer function matrix of hybrid multi-terminal HVDC system with flexible adaptability for different operation modes," *International Journal of Electrical Power & Energy Systems*, vol. 116, Mar. 2020, doi: 10.1016/j.ijepes.2019.105584.

[9] S. Asvapoositkul and R. Preece, "Impact of HVDC dynamic modelling on power system small signal stability assessment," *International Journal of Electrical Power & Energy Systems*, vol. 123, Dec. 2020, doi: 10.1016/j.ijepes.2020.106327.

[10] M. Benasla, T. Allaoui, M. Brahami, V. K. Sood, and M. Denaï, "Power system security enhancement by HVDC links using a closed-loop emergency control," *Electric Power Systems Research*, vol. 168, pp. 228–238, Mar. 2019, doi: 10.1016/j.epsr.2018.12.002.

[11] X. Chu and H. Lv, "Coupling characteristic analysis and a fault pole detection scheme for single-circuit and double-circuit HVDC transmission lines," *Electric Power Systems Research*, vol. 181, Apr. 2020, doi: 10.1016/j.epsr.2019.106179.

[12] S. Mirsaeidi, X. Dong, and D. M. Said, "A fault current limiting approach for commutation failure prevention in LCC-HVDC transmission systems," *IEEE Transactions on Power Delivery*, vol. 34, no. 5, pp. 2018–2027, Oct. 2019, doi: 10.1109/TPWRD.2019.2907558.

[13] I. M. Ginarsa, A. B. Muljono, I. M. A. Nrartha, and Sultan, "Transient response improvement of direct current using supplementary control based on anfis for rectifier in HVDC," *International Journal of Power Electronics and Drive Systems (IJPEDS)*, vol. 11, no. 4, pp. 2107–2115, 2020, doi: 10.11591/ijpeds.v11.i4.pp2107-2115.

[14] Y. Xu, W. Bai, S. Zhao, J. Zhang, and Y. Zhao, "Mitigation of forced oscillations using VSC-HVDC supplementary damping control," *Electric Power Systems Research*, vol. 184, Jul. 2020, doi: 10.1016/j.epsr.2020.106333.

[15] Y. Wang, C. Guo, and C. Zhao, "A novel supplementary frequency-based dual damping control for VSC-HVDC system under weak AC grid," *International Journal of Electrical Power and Energy Systems*, vol. 103, no. May, pp. 212–223, 2018, doi: 10.1016/j.ijepes.2018.05.033.

[16] E. Tsotsopoulou, X. Karagiannis, T. Papadopoulos, A. Chrysochos, A. Dyśko, and D. Tzelepis, "Protection scheme for multi-terminal HVDC system with superconducting cables based on artificial intelligence algorithms," *International Journal of Electrical Power & Energy Systems*, vol. 149, Jul. 2023, doi: 10.1016/j.ijepes.2023.109037.

[17] B. Shang, G. Luo, M. Li, Y. Liu, and J. Hei, "Transfer learning-based fault location with small datasets in VSC-HVDC," *International Journal of Electrical Power and Energy Systems*, vol. 151, no. January, Art. no. 109131, 2023, doi: 10.1016/j.ijepes.2023.109131.

[18] S. Ankar and A. Yadav, "ANN-based protection scheme for bipolar CSC-based HVDC transmission line," in *2019 Innovations in Power and Advanced Computing Technologies (i-PACT)*, Mar. 2019, pp. 1–5, doi: 10.1109/i-PACT44901.2019.8960148.

[19] Y. Tang, H. He, Z. Ni, J. Wen, and T. Huang, "Adaptive modulation for DFIG and STATCOM with high-voltage direct current transmission," *IEEE Transactions on Neural Networks and Learning Systems*, vol. 27, no. 8, pp. 1762–1772, Aug. 2016, doi: 10.1109/TNNLS.2015.2504035.

[20] B. Abdelkrim and Y. Merzoug, "Robust stability power in the transmission line with the use of a UPFC system and neural controllers based adaptive control," *International Journal of Power Electronics and Drive Systems (IJPEDS)*, vol. 10, no. 3, pp. 1281–1296, Sep. 2019, doi: 10.11591/ijpeds.v10.i3.pp1281-1296.

[21] S. Azizi, M. H. Asemani, N. Vafamand, S. Mobayen, and A. Fekih, "Adaptive neural network linear parameter-varying control of shipboard direct current microgrids," *IEEE Access*, vol. 10, no. June, pp. 75825–75834, 2022, doi: 10.1109/ACCESS.2022.3191385.

[22] P. Sharma, S. Singh, and V. Pahwa, "Implementation of ANFIS based controller on IG wind farm for improved performance," *IAES International Journal of Robotics and Automation (IJRA)*, vol. 8, no. 2, pp. 94–104, Jun. 2019, doi: 10.11591/ijra.v8i2.pp94-104.

[23] G. Joshi and A. J. P. Pius, "ANFIS controller for vector control of three phase induction motor," *Indonesian Journal of Electrical Engineering and Computer Science (IJEECS)*, vol. 19, no. 3, pp. 1177–1185, 2020, doi: 10.11591/ijeecs.v19.i3.pp1177-1185.

[24] K. W. Nasser, S. J. Yaqoob, and Z. A. Hassoun, "Improved dynamic performance of photovoltaic panel using fuzzy logic-MPPT algorithm," *Indonesian Journal of Electrical Engineering and Computer Science (IJEECS)*, vol. 21, no. 2, pp. 617–624, 2020, doi: 10.11591/ijeecs.v21.i2.pp617-624.

[25] I. M. Ginarsa, I. M. A. Nrartha, A. B. Muljono, and S. Nababan, "Strategy to reduce transient current of inverter-side on an average value model high voltage direct current using adaptive neuro-fuzzy inference system controller," *International Journal of Electrical and Computer Engineering (IJECE)*, vol. 12, no. 5, pp. 4790–4800, 2022, doi: 10.11591/ijece.v12i5.pp4790-4800.

[26] I. M. Ginarsa, A. Soeprijanto, and M. H. Purnomo, "Controlling chaos and voltage collapse using an ANFIS-based composite controller-static var compensator in power systems," *International Journal of Electrical Power & Energy Systems*, vol. 46, pp. 79–88, Mar. 2013, doi: 10.1016/j.ijepes.2012.10.005.

[27] A. B. Muljono, I. M. Ginarsa, I. M. A. Nrartha, and A. Dharma, "Coordination of adaptive neuro fuzzy inference system (ANFIS) and type-2 fuzzy logic system-power system stabilizer (T2FLS-PSS) to improve a large-scale power system stability," *International Journal of Electrical and Computer Engineering (IJECE)*, vol. 8, no. 1, pp. 76–86, Feb. 2018, doi: 10.11591/ijece.v8i1.pp76-86.

[28] G. Kamalapur and M. S. Aspalli, "Direct torque control and dynamic performance of induction motor using fractional order fuzzy logic controller," *International Journal of Electrical and Computer Engineering (IJECE)*, vol. 13, no. 4, pp. 3805–3816, Aug. 2023, doi: 10.11591/ijece.v13i4.pp3805-3816.

[29] E. H. Karam, N. A. Al-awad, and N. S. Abdul-jaleel, "Design nonlinear model reference with fuzzy controller for nonlinear SISO second order systems," *International Journal of Electrical and Computer Engineering (IJECE)*, vol. 9, no. 4, pp. 2491–2502, 2019, doi: 10.11591/ijece.v9i4.pp2491-2402.

[30] S. Wahsh, Y. Ahmed, and A. Elzahab, "Implementation of type-2 fuzzy logic controller in PMSM drives using DSP," *International Journal of Power Electronics and Drive Systems (IJPEDS)*, vol. 9, no. 3, pp. 1098–1105, Sep. 2018, doi: 10.11591/ijpeds.v9.i3.pp1098-1105.

[31] S. J. Hong, S. W. Hyun, K. M. Kang, J. H. Lee, and C. Y. Won, "Improvement of transient state response through feedforward compensation method of AC/DC power conversion system (PCS) based on space vector pulse width modulation (SVPWM)," *Energies*, vol. 11, no. 6, 2018, doi: 10.3390/en11061468.

[32] P. Suresh *et al.*, "Reduction of transients in switches using embedded machine learning," *International Journal of Power Electronics and Drive Systems (IJPEDS)*, vol. 11, no. 1, pp. 235–241, 2020, doi: 10.11591/ijpeds.v11.i1.pp235-241.

[33] S. Wu, Y. Kobori, N. Tsukiji, and H. Kobayashi, "Transient response improvement of DC-DC buck converter by a slope adjustable triangular wave generator," *IEICE Transactions on Communications*, vol. E98.B, no. 2, pp. 288–295, 2015, doi: 10.1587/transcom.E98.B.288.

[34] B. Butterfield, "Optimizing transient response of internally compensated dc-dc converters with feedforward capacitor," Texas Instruments, 2017.

[35] K. Sato, T. Sato, and M. Sonehara, "Transient response improvement of digitally controlled DC-DC converter with feedforward

        compensation," in *2017 IEEE International Telecommunications Energy Conference (INTELEC)*, Oct. 2017, pp. 609–614, doi: 10.1109/INTLEC.2017.8214205.

[36] A. Cheraghalipour, M. Hajiaghaei-Keshteli, and M. M. Paydar, "Tree growth algorithm (TGA): A novel approach for solving optimization problems," *Engineering Applications of Artificial Intelligence*, vol. 72, no. April, pp. 393–414, 2018, doi: 10.1016/j.engappai.2018.04.021.

[37] H. T. Sadeeq and A. M. Abdulazeez, "Giant trevally optimizer (GTO): A novel metaheuristic algorithm for global optimization and challenging engineering problems," *IEEE Access*, vol. 10, pp. 121615–121640, 2022, doi: 10.1109/ACCESS.2022.3223388.

[38] H. T. Sadeeq and A. M. Abdulazeez, "Improved Northern Goshawk optimization algorithm for global optimization," in *ICOASE 2022 - 4th International Conference on Advanced Science and Engineering*, 2022, no. March, pp. 89–94, doi: 10.1109/ICOASE56293.2022.10075576.

[39] I. Strumberger, E. Tuba, N. Bacanin, and M. Tuba, "Dynamic tree growth algorithm for load scheduling in cloud environments," in *2019 IEEE Congress on Evolutionary Computation, CEC 2019 - Proceedings*, 2019, pp. 65–72, doi: 10.1109/CEC.2019.8790014.

[40] M. Najafi Ashtiani, A. Toopshekan, F. Razi Astaraei, H. Yousefi, and A. Maleki, "Techno-economic analysis of a grid-connected PV/battery system using the teaching-learning-based optimization algorithm," *Solar Energy*, vol. 203, no. July 2019, pp. 69–82, 2020, doi: 10.1016/j.solener.2020.04.007.

[41] J. Zhang, M. Xiao, L. Gao, and Q. Pan, "Queuing search algorithm: A novel metaheuristic algorithm for solving engineering optimization problems," *Applied Mathematical Modelling*, vol. 63, pp. 464–490, 2018, doi: 10.1016/j.apm.2018.06.036.

[42] S. Talatahari, M. Azizi, M. Tolouei, B. Talatahari, and P. Sareh, "Crystal structure algorithm (CryStAl): A Metaheuristic optimization method," *IEEE Access*, vol. 9, pp. 71244–71261, 2021, doi: 10.1109/ACCESS.2021.3079161.

[43] T. Ma, "Two-stage economic dispatch optimization for integrated energy system using improved brain storm optimization algorithm," *2019 IEEE Innovative Smart Grid Technologies - Asia (ISGT Asia)*, pp. 2968–2973, 2019.

[44] K. Lenin, "Power loss reduction by chaotic based predator-prey brain storm optimization algorithm," *International Journal of Applied Power Engineering (IJAPE)*, vol. 9, no. 3, pp. 218–222, Dec. 2020, doi: 10.11591/ijape.v9.i3.pp218-222.

[45] K. Lenin, "Minimization of real power loss by enhanced teaching learning based optimization algorithm," *IAES International Journal of Robotics and Automation (IJRA)*, vol. 9, no. 1, pp. 1–5, Mar. 2020, doi: 10.11591/ijra.v9i1.pp1-5.

[46] Rekha and S. C. Byalihal, "Optimal allocation of solar and wind distributed generation using particle swarm optimization technique," *International Journal of Electrical and Computer Engineering (IJECE)*, vol. 13, no. 1, pp. 229–237, 2023, doi: 10.11591/ijece.v13i1.pp229-237.

[47] M. Tavakoli, E. Pouresmaeil, J. Adabi, R. Godina, and J. P. S. Catalão, "Load-frequency control in a multi-source power system connected to wind farms through multi terminal HVDC systems," *Computers & Operations Research*, vol. 96, pp. 305–315, Aug. 2018, doi: 10.1016/j.cor.2018.03.002.

[48] N. Priyadarshi, S. Padmanaban, J. B. Holm-Nielsen, F. Blaabjerg, and M. S. Bhaskar, "An experimental estimation of hybrid ANFIS–PSO-based MPPT for PV grid integration under fluctuating sun irradiance," *IEEE Systems Journal*, vol. 14, no. 1, pp. 1218–1229, Mar. 2020, doi: 10.1109/JSYST.2019.2949083.

[49] A. P. Bheemasenarao and S. C. Byalihal, "Optimal protective relaying scheme of distributed generation connected distribution network using particle swarm optimization-gravitational search algorithm technique," *International Journal of Electrical and Computer Engineering (IJECE)*, vol. 13, no. 3, pp. 2568–2578, 2023, doi: 10.11591/ijece.v13i3.pp2568-2578.

[50] M. Ahmed, M. A. Ebrahim, H. S. Ramadan, and M. Becherif, "Optimal genetic-sliding mode control of VSC-HVDC transmission systems," *Energy Procedia*, vol. 74, pp. 1048–1060, Aug. 2015, doi: 10.1016/j.egypro.2015.07.743.

[51] G. M. Sivasubramanian and M. Narayanamurthy, "Implementation of PWM AC chopper controller for capacitor run induction motor drive via bacterial foraging optimization algorithm," *International Journal of Reconfigurable and Embedded Systems (IJRES)*, vol. 9, no. 3, pp. 169–177, Nov. 2020, doi: 10.11591/ijres.v9.i3.pp169-177.

[52] O. Zebua, I. M. Ginarsa, and I. M. A. Nartha, "GWO-based estimation of input-output parameters of thermal power plants," *Telkomnika (Telecommunication Computing Electronics and Control)*, vol. 18, no. 4, pp. 2235–2244, 2020, doi: 10.12928/TELKOMNIKA.V18I4.12957.

[53] S. Yadav, H. R. Chamorro, W. C. Flores, and R. K. Mehta, "Investigation of improved thermal dissipation of ±800 kV converter transformer bushing employing nano-hexagonal boron nitride paper using FEM," *IEEE Access*, vol. 9, pp. 149196–149217, 2021, doi: 10.1109/ACCESS.2021.3124917.

[54] S. Casoria, "Thyristor-based HVDC transmission system," Hydro-Quebec, 2013.

[55] S. Mirjalili, S. M. Mirjalili, and A. Lewis, "Grey wolf optimizer," *Advances in Engineering Software*, vol. 69, pp. 46–61, Mar. 2014, doi: 10.1016/j.advengsoft.2013.12.007.

[56] MATLAB, "MATLAB Simulink." The Mathworks, Old Baltimore Pike, 2013.

BIOGRAPHIES OF AUTHORS

I Made Ginarsa 🆔 🔳 🆂🅲 ↻ received the B.Eng. (1997), M.T. (2001) and Ph.D (2012) degrees in electrical engineering from Udayana, Universitas Gadjah Mada, and Institut Teknologi Sepuluh Nopember, Indonesia, respectively. He is a lecturer at the Department of Electrical Engineering, University of Mataram. In 2010 he was a member of EPS Lab., Kumamoto Univ. His research is voltage and dynamic stability, nonlinear dynamic, application of artificial intelligence in high voltage direct current and power systems. He was the institution of engineers Indonesia member, author, co-author and invited reviewer on national and international publications. He can be contacted at email: kadekgin@unram.ac.id.

I Made Ari Nrartha 🆔 � SC ↻ received in B.Eng and M.Eng in electrical engineering from Institute Technology Sepuluh Nopember, Surabaya and Gadjah Mada University, Yogyakarta Indonesia, in 1997 and 2001, respectively. Since 1999 he was a lecturer at Electrical Eng., University of Mataram. His research interests are power system dynamic and stability, transmission and distribution, optimization, power quality and artificial intelligent application in power systems. He was the institution of engineers Indonesia member, active author and co-author research papers in national and international journal, and served as editorial board in Dielektrika Journal. He can be contacted at email: nrartha@unram.ac.id.

Agung Budi Muljono 🆔 � SC ↻ received the B.Eng. and M.Eng. in electrical engineering from Malang Institute of Technology (1996) and UGM (2000), respectively. He was IEEE, FORTEI members, author, co-author papers and served as editorial board in Dielektrika Journal. His research interests include transmission and distribution, dynamic and stability, artificial intelligent application, and energy planning and distributed generation in power systems. He was the institution of engineers Indonesia member, author, co-author papers and served as editorial board in Dielektrika Journal. He can be contacted at email: agungbm@unram.ac.id.

Osea Zebua 🆔 � SC ↻ received the B.Eng. (1997) and M.Eng. (2001) degree in electrical engineering from Sumatera Utara University and Gadjah Mada University, Indonesia, respectively, He has been a lecturer of electrical power engineering with University of Lampung, Indonesia, since 2001. His research interests include power system operation, transmission and distribution, optimization, power quality, artificial intelligent application in power systems. He was an active author and co-author research papers in national and international journal. He can be contacted at email: osea.zebua@eng.unila.ac.id.